ARMA 21–1653

Different Numerical Methods for Naturally Fractured Reservoir Simulation with EDFM

Yu, Wei
Sim Tech LLC, Houston, Texas, USA
Xing, Yuzhong; Cheng, Muwei; Chen, Pengyu
The Research Institute of Petroleum Exploration and Development CNPC, Beijing, China
Fiallos Torres, Mauricio Xavier; Mao, Zhenyu; Miao, Jijun
Sim Tech LLC, Houston, Texas, USA

This paper was prepared for presentation at the 55th US Rock Mechanics/Geomechanics Symposium held in Houston, Texas, USA, 20-23 June 2021. This paper was selected for presentation at the symposium by an ARMA Technical Program Committee based on a technical and critical review of the paper by a minimum of two technical reviewers. The material, as presented, does not necessarily reflect any position of ARMA, its officers, or members. Electronic reproduction, distribution, or storage of any part of this paper for commercial purposes without the written consent of ARMA is prohibited. Permission to reproduce in print is restricted to an abstract of not more than 200 words; illustrations may not be copied. The abstract must contain conspicuous acknowledgement of where and by whom the paper was presented.

ABSTRACT: Accurate and efficient simulation of multi-phase flow in naturally fractured reservoirs with complex natural fractures is very important for economic development. There are several key methods to perform reservoir simulation with natural fractures such as dual porosity dual permeability (DPDK), embedded discrete fracture model (EDFM) and the combination of EDFM and DPDK. However, each method has its advantages and disadvantages. DPDK cannot model natural fractures explicitly and accurately. However, DPDK is usually more efficient than EDFM. EDFM is more accurate for fracture modeling and simulation. However, the EDFM needs to generate more additional fracture cells than DPDK when modeling large number of fractures, leading to lower computational efficiency than DPDK. In this study, we benchmarked four different methods using the actual field data including EDFM, DPDK, EDFM used to model large fractures and small fractures are upscaled to single porosity model, and EDFM used to model large fractures and small fractures are upscaled to DPDK. The accuracy and efficiency were systematically compared. This study provides key insights for naturally fractured reservoir simulation.

1. INTRODUCTION

The presence of a large number of three-dimensional complex natural fractures plays an important role in economic development of naturally fractured oil and gas reservoirs. An efficient reservoir simulation method to model the effect of such complex fractures effectively and accurately on well performance is needed.

Traditionally, the method of dual porosity and dual permeability (DPDK) is often used to model complex natural fractures with high fracture density (Warren and Root, 1963; Kazemi et al, 1976; Blaskovich et al., 1983; Hill and Thomas, 1985). However, this method cannot handle natural fractures explicitly and accurately. In order to properly model any complex natural fractures, we have developed a non-intrusive embedded discrete fracture model (EDFM) method (Xu et al., 2017, 2019; Xu and Sepehrnoori, 2019; Sepehrnoori et al., 2020). It works with both in-house and third-party reservoir simulators with the capability of non-neighboring connections (NNCs) to model fractures using structured grids without the need of unstructured grids. The comparison between EDFM and DPDK methods with the real field data has not been well investigated.

In this study, we build a field-scale single-well carbonate gas reservoir model with complex natural fractures. Four different methods, including EDFM, DPDK, EDFM used to model large fractures and small fractures are upscaled to single porosity, and EDFM used to model large fractures and small fractures are upscaled to DPDK, were systematically compared through performing history matching with field production data.

2. DIFFERENT FRACTURED RESERVOIR SIMULATION METHODS

Four methods are applied to model and simulate multi-phase flow of complex natural fracture networks in the following simulation studies.

Method 1 is EDFM. All complex natural fractures are modeled using the EDFM method. Fig. 1 shows the key concept of the non-intrusive EDFM method to model 3D complex fractures using simple structured cells. As can be seen, the complex fractures are directly embedded into matrix cells in the physical domain. After checking the intersection of complex fractures and matrix cells, two groups of cells are generated in the computational domain, including matrix cells and fracture cells. Multi-phase fluid flow between matrix and fracture cells is

modeled and simulated based on the NNCs and transmissibility. More details can be found in the work by Xu et al. (2017, 2019).

Method 2 is DPDK. All complex natural fractures are upscaled to DPDK.

Method 3 is the combination of EDFM and upscaled single porosity model. All complex natural fractures except cross-wellbore fractures will be divided into two groups based on the fracture size. Large natural fractures will be modeled using the EDFM method while small natural fractures will be upscaled to single porosity model by increasing matrix cell porosity and permeability when the cell includes natural fractures.

Method 4 is the combination of EDFM and DPDK. All complex natural fractures except cross-wellbore fractures will be divided into two groups based on the fracture size. Large natural fractures will be modeled using the EDFM method while small natural fractures will be upscaled to DPDK.

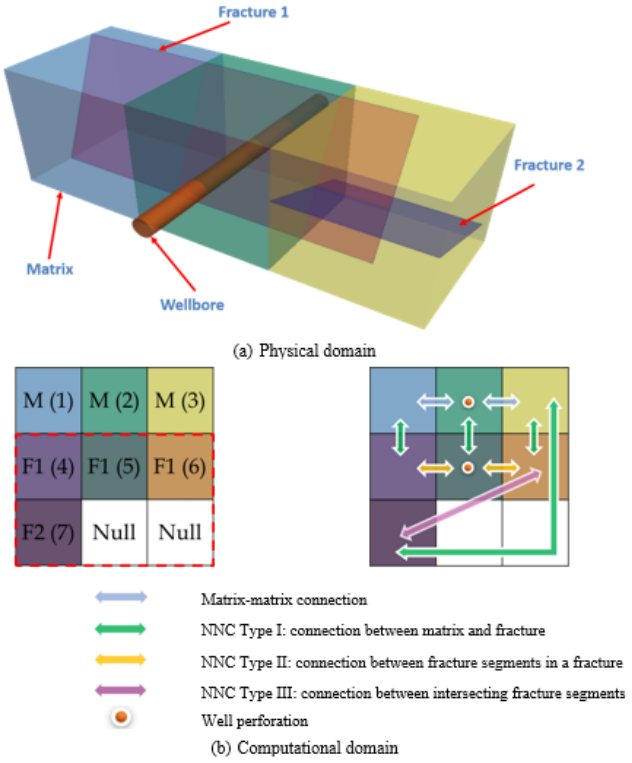

Fig. 1. Key concept of the non-intrusive EDFM method to model 3D complex natural fractures (Xu et al., 2017).

3. COMPARISON OF DIFFERENT METHODS

We built a field-scale actual carbonate reservoir model with corner point including a single vertical well and complex natural fractures, as shown in Fig. 2. As can be seen, three different groups of natural fractures are distinguished and modeled separately including cross-wellbore natural fractures (0-50 m), nearby wellbore natural fractures (50-1000 m), and natural fractures away from wellbore (larger than 1000 m). The number of natural fractures for the three group of natural fractures is 186, 1262, and 13619, respectively. In total, there are 15067 natural fractures. The natural fracture length, height, azimuth, and dip angle distribution is shown in Fig. 3. The reservoir model dimension is 2000 m × 2000 m × 200 m, which corresponds to reservoir length, width, and thickness, respectively. Gas-water two phase flow is considered and simulated. The natural fracture distribution was generated based on the available information such as seismic, outcrop, and image log etc. The key reservoir, fracture, and fluid properties for the following reservoir simulations are summarized in Table 1.

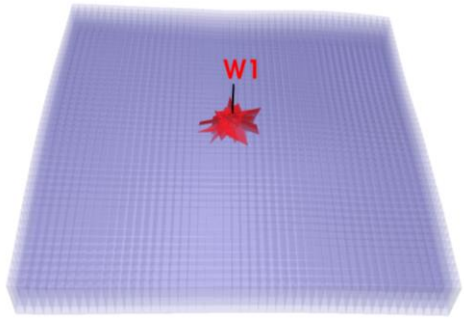

(a) Cross-wellbore natural fractures (0-50 m)

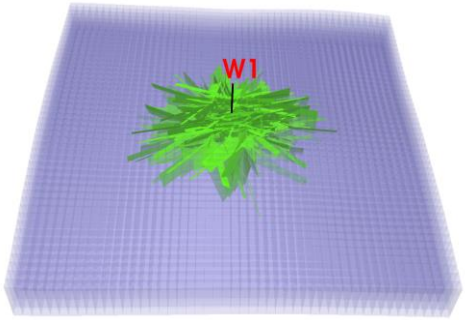

(b) Nearby wellbore natural fractures (50-1000 m)

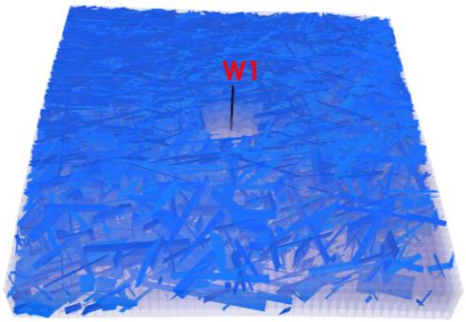

(c) Natural fractures away from wellbore (larger than 1000 m)

Fig. 2. A field-scale reservoir model with a vertical well and complex natural fractures.

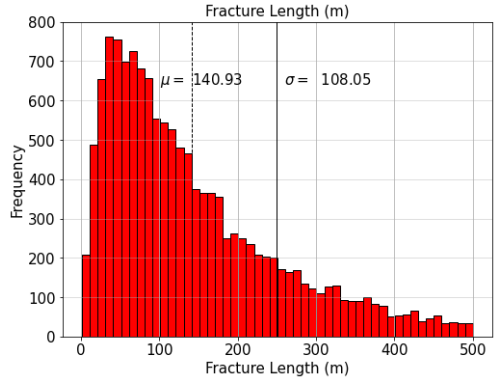

(a) Fracture length distribution

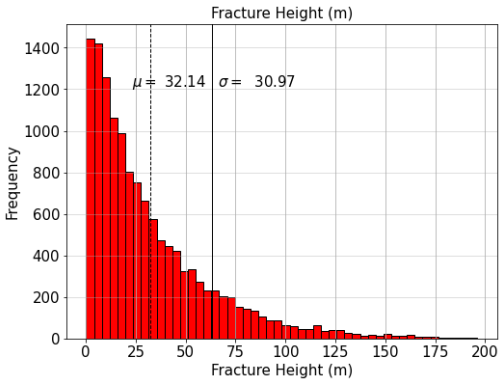

(b) Fracture height distribution

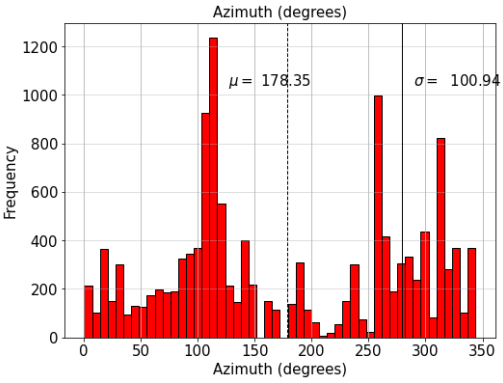

(c) Fracture azimuth distribution

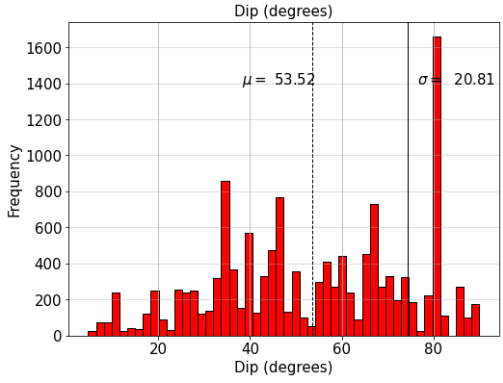

(d) Fracture dip distribution

Fig. 3. Statistical information of fracture length, height, azimuth, and dip angle of all the natural fractures.

Table 1. Key reservoir, fracture, and fluid properties used for reservoir simulation in this study

Parameter	Value	Unit
Reservoir size	2000×2000×200	m
Grid size	40×40×50	m
Reservoir depth	2880	m
Rock compressibility	3.0×10^{-5}	$bars^{-1}$
Average reservoir permeability	0.1	md
Reservoir porosity	8%	-
Residual water saturation	43.75%	-
Initial reservoir pressure	584.7	bars
Fracture conductivity	0.01-10	md-m
Fracture aperture	0.001-0.01	m

There are around 1600 days of actual production data available for history matching and calibration of the reservoir model and fracture properties. During the history matching process, the measured gas flow rate was applied for the reservoir simulation constraint and flowing bottomhole pressure and water flow rate was the history-matching targets. The fracture conductivity of three different natural fracture groups was the main tuning parameter.

First, we applied the EDFM method to perform history matching. After directly embedding 15067 natural fractures in the 9604 matrix cells, 142100 fracture cells were generated, resulting in a total number of 151704 cells for the final reservoir model including matrix and natural fractures. The history matching results are shown in Fig. 4. It can be seen that great matches of bottomhole pressure and water intrusion were obtained. The CPU time of the single model run with the EDFM method is about 217 seconds.

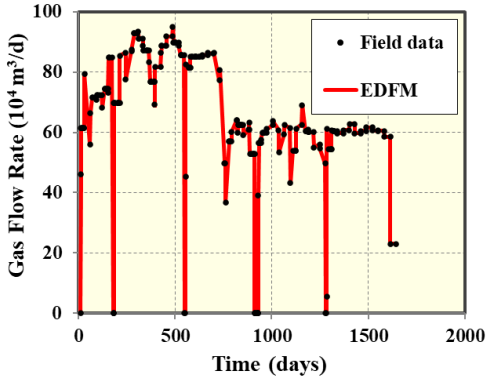

(a) Gas flow rate used for simulation constraint

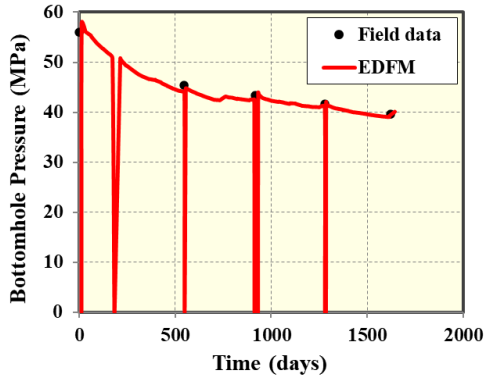

(b) Flowing bottomhole pressure

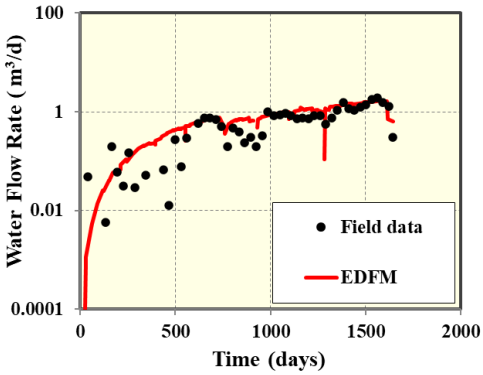

(c) Water flow rate

Fig. 4. Comparison of simulation results with field production data using the EDFM method.

Comparison of natural fracture conductivity before and after history matching is shown in Fig. 5. As shown, the initial natural fracture conductivity is uniform with 1 md-m. After history matching, the conductivity of cross-wellbore natural fractures, nearby and away from wellbore natural fractures is 10 md-m, 1 md-m, and 0.01 md-m, respectively. In addition, the aperture of cross-wellbore fractures is 0.01 m and the aperture of the other fractures is 0.001 m.

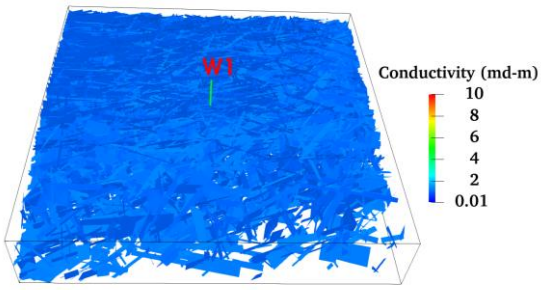

(a) Before history matching

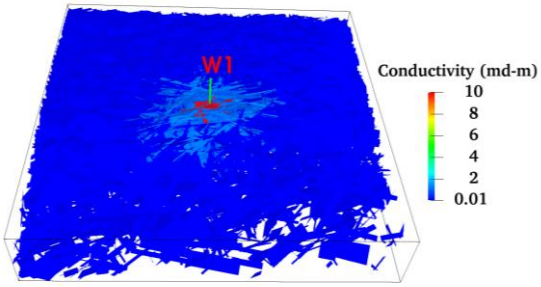

(b) After history matching

Fig. 5. Comparison of natural fracture conductivity before and after history matching.

Comparisons of natural fracture pressure and water saturation distribution before and after history matching are shown in Figs. 6 and 7, respectively. There is an obvious and strong pressure drawdown nearby the wellbore region. Also, the water saturation in the complex natural fractures can be clearly observed using the EDFM method.

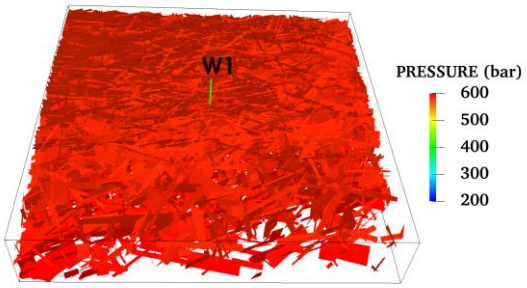

(a) Before history matching

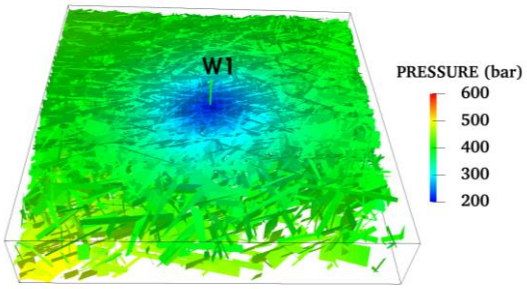

(b) After history matching

Fig. 6. Comparison of natural fracture pressure before and after history matching.

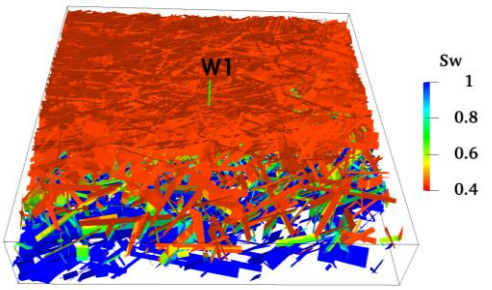

(a) Before history matching

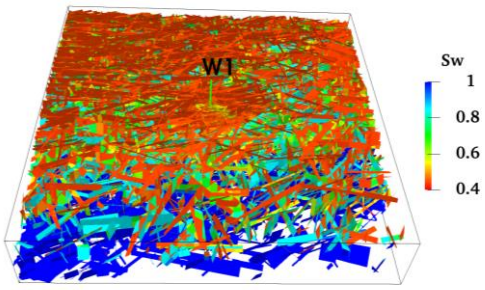

(b) After history matching

Fig. 7. Comparison of natural fracture water saturation before and after history matching.

In addition, comparison of natural fracture water intrusion process before and after history matching is shown in Fig. 8. The non-uniform water intrusion from bottom water to wellbore through complex natural fractures is clearly observed.

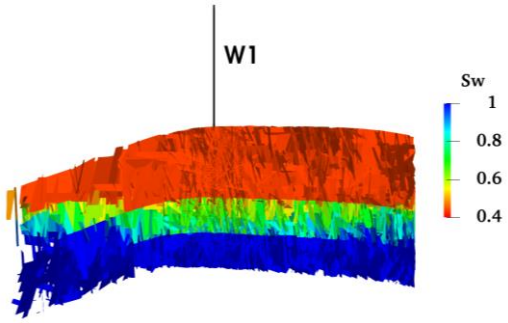

(a) Before history matching

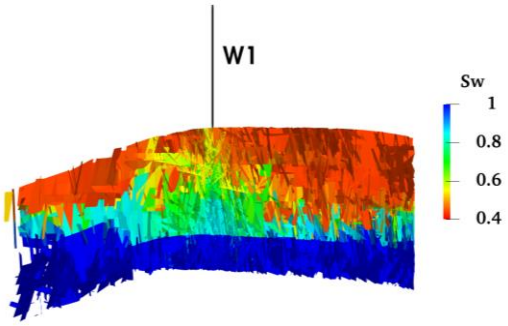

(b) After history matching

Fig. 8. Comparison of natural fracture water intrusion process before and after history matching.

Next, we applied the DPDK method perform history matching and compare the results with the EDFM method. Fig. 9 presents the upscaled fracture permeability, porosity and sigma value distribution with the DPDK method based on the fracture properties calibrated with production data with the EDFM method. The comparison of history matching results between the EDFM and DPDK methods is shown in Fig. 10. The simulation results show that the bottomhole pressure of the DPDK method is a little bit higher than the EDFM method. However, the water flow rate of the DPDK method is much larger than the EDFM method and the field data, especially after around 400 days of production. The main reason is that the DPDK method cannot accurately capture the real connection of complex natural fracture networks. In this case study, the DPDK method overestimate the natural fracture connection. There are more cross-wellbore natural fractures, resulting in larger upscaled fracture permeability and faster water intrusion process, as shown in Fig. 11. The CPU time of the single model run with the DPDK method is about 35 seconds, which is much faster than the EDFM method due to the smaller number of fracture cells of 9604 to model fractures, which is the same as the number of matrix cells.

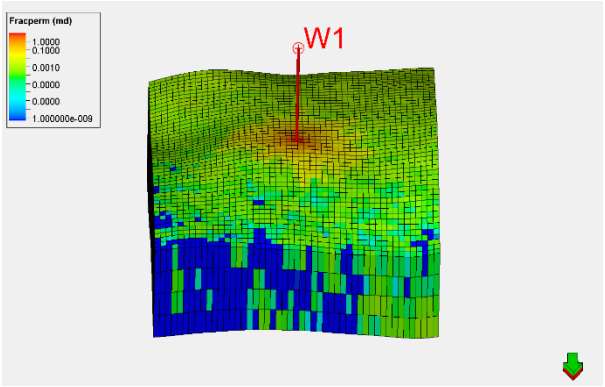

(a) Upscaled fracture permeability

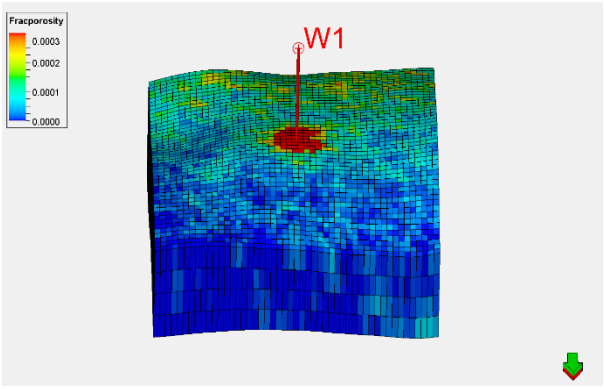

(b) Upscaled fracture porosity

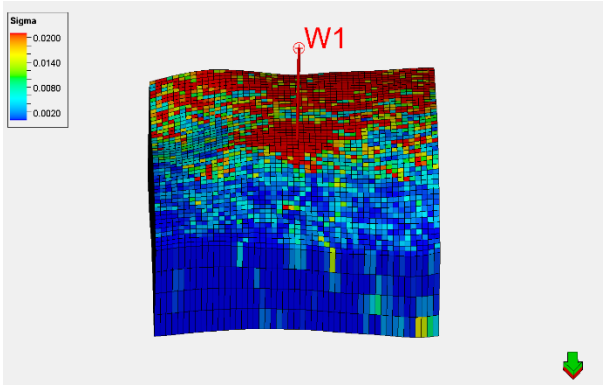

(c) Upscaled sigma

Fig. 9. Upscaled fracture permeability, porosity, and sigma distribution with the DPDK method based on the fracture properties calibrated with production data with the EDFM method.

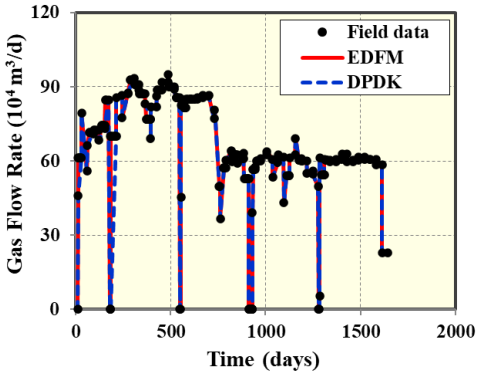

(a) Gas flow rate used for simulation constraint

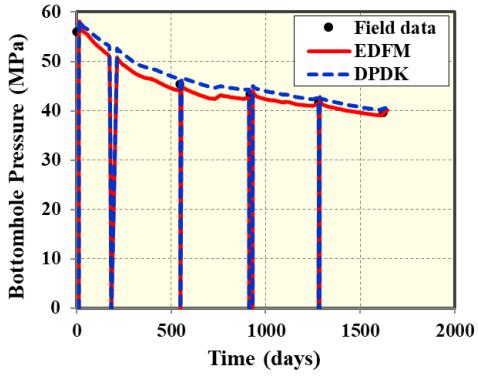

(b) Flowing bottomhole pressure

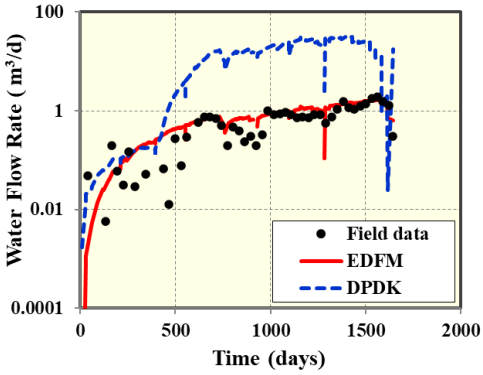

(c) Water flow rate

Fig. 10. Comparison of history matching results between the EDFM and DPDK methods.

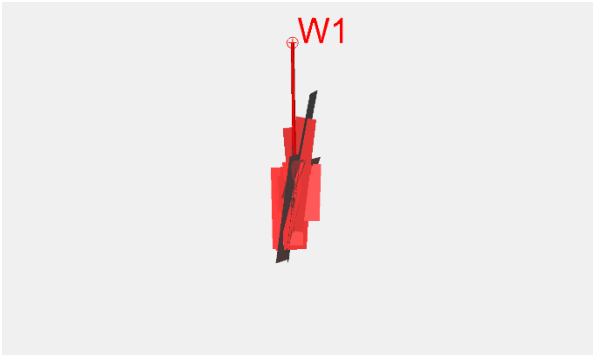

(a) Cross-wellbore natural fractures before upscaling

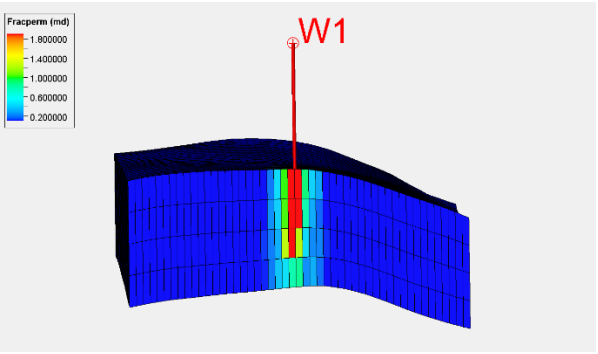

(b) Upscaled fracture permeability nearby wellbore

Fig. 11. Upscaled fracture permeability for the cross-wellbore natural fractures using the DPDK method.

For the third and fourth method, we separate natural fractures except cross-wellbore fractures into two groups based on the fracture length of 50 m, as shown in Fig. 12. One group of small fractures with fracture length less than 50 m and the number is 3008. Another one is big fractures with fracture length larger than 50 m and the number is 11918. For the third method using the combination of EDFM and upscaled single porosity model, the small natural fractures were upscaled into matrix grids with increasing matrix porosity and permeability, as shown in Fig. 13. For the fourth method of using the combination of EDFM and DPDK, the small natural fractures were upscaled to fracture permeability, porosity, and sigma, as shown in Fig. 14. For both methods, the big natural fractures were modeled by the EDFM method. The CPU time of the third and fourth methods is about 191 seconds and 222 seconds, respectively. Comparison of history matching results between four different methods is shown in Fig. 15. It can be seen that the third method has similar match with the EDFM method, which is better the fourth method. In addition, the computational efficiency of the third method is faster than the EDFM method due to less fracture cells generated from big fractures, which is 132496. Hence, the method of using the combination of EDFM and upscaled single porosity model is the best one in this study based on the accuracy and efficiency.

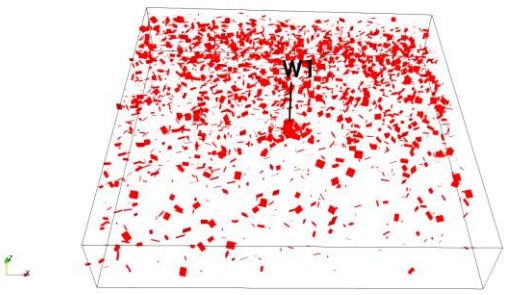

(a) 3008 small natural fractures with length less than 50 m

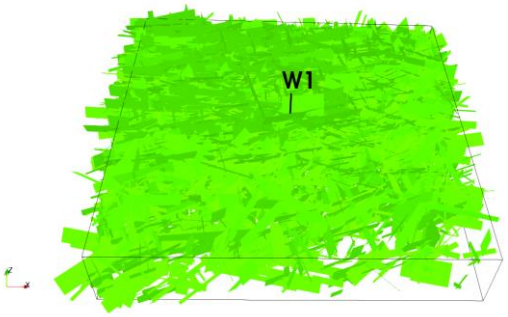

(b) 12059 big natural fractures with length larger than 50 m

Fig. 12. Small and big natural fracture distribution based on the critical fracture length of 50 m.

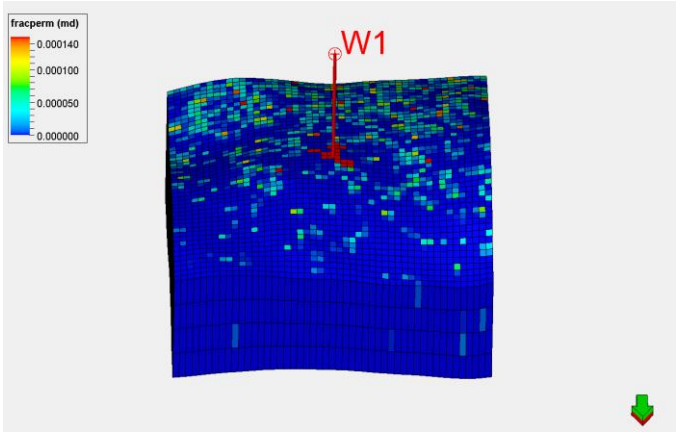

(a) Upscaled matrix permeability for small fractures

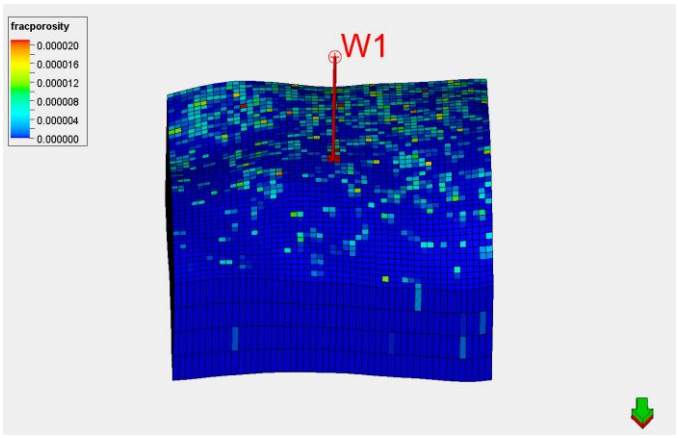

(b) Upscaled matrix porosity for small fractures

Fig. 13. The third method using the combination of EDFM and upscaled single porosity model.

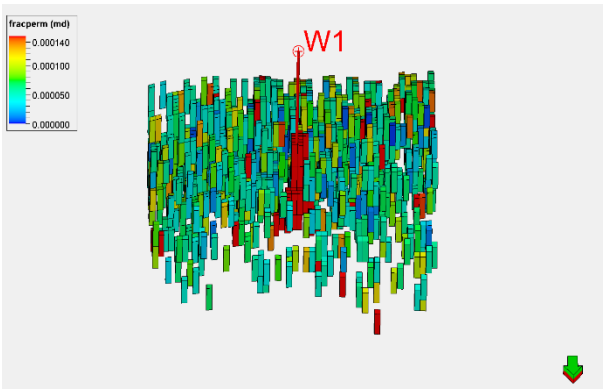

(a) Upscaled fracture permeability for small fractures

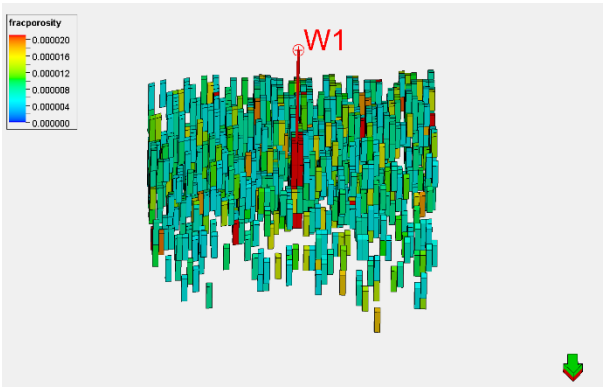

(b) Upscaled fracture porosity for small fractures

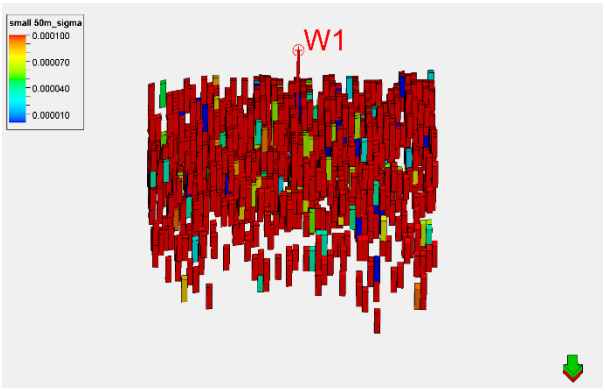

(c) Upscaled sigma for small fractures

Fig. 14. The fourth method using the combination of EDFM and DPDK.

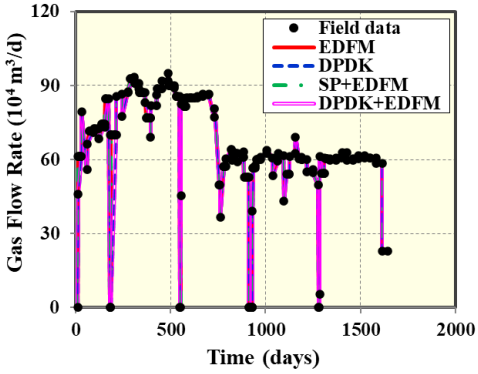

(a) Gas flow rate used for simulation constraint

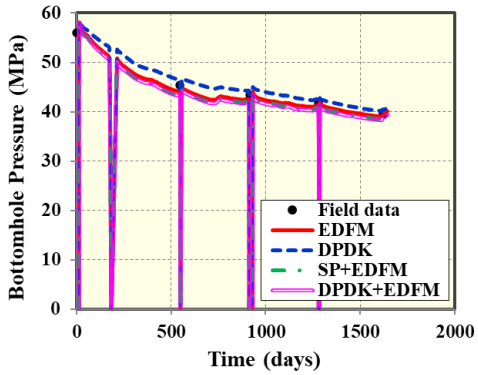

(b) Flowing bottomhole pressure

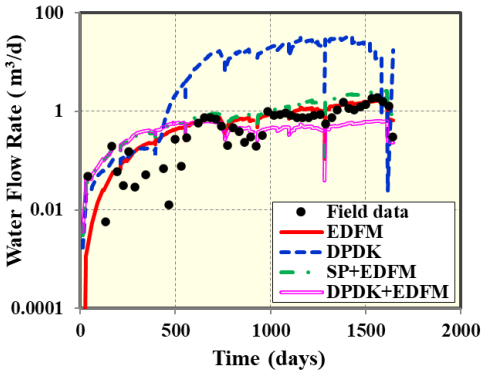

(c) Water flow rate

Fig. 15. Comparison of history matching results between four different methods.

4. CONCLUSIONS

We compared four different methods including EDFM, DPDK, the combination of EDFM and upscaled single porosity model, and the combination of EDFM and DPDK using field production data. The following conclusions can be drawn from this study:

(1) The EDFM method performs better than the DPDK method for modeling complex natural fractures based on history matching results.

(2) The DPDK method predicts more water intrusion than the EDFM method due to its overestimation of fracture permeability of cross-wellbore natural fractures connection.

(3) The method of combination of EDFM and upscaled single porosity model performs better than the EDFM method based on accuracy and efficiency, which is also better than the method of combination of EDFM and DPDK.

REFERENCES

1. Blaskovich, F.T., Cain, G.M., Sonier, F., Waldren, D., and Webb, S.J. 1983. A Multicomponent Isothermal System for Efficient Reservoir Simulation. Paper SPE 11480, *presented at the Middle East Oil Technical Conference and Exhibition*, 14-17 March, Manama, Bahrain.
2. Hill, A.C., and Thomas, G.W. 1985. A New Approach for Simulating Complex Fractured Reservoirs. Paper SPE 13537, *presented at the Middle East Oil Technical Conference and Exhibition*, 11-14 March, Bahrain.
3. Kazemi, H., Merrill, L.S., Jr., Porterfield, K.L., and Zeman, P.R. 1976. Numerical Simulation of Water-Oil Flow in Naturally Fractured Reservoirs. *SPE Journal*, 16 (6): 317-326.
4. Sepehrnoori, K., Xu, Y., and Yu, W. 2020. Embedded Discrete Fracture Modeling and Application in Reservoir Simulation, 1st Ed., Publisher: Elsevier, Cambridge, USA. ISBN: 978-0128196885.
5. Warren, J.E., and Root, P.J. 1963. The Behavior of Naturally Fractured Reservoirs. *SPE Journal*, 3 (3): 245-255.
6. Xu, Y., and Sepehrnoori, K. 2019. Development of an Embedded Discrete Fracture Model for Field-Scale Reservoir Simulation with Complex Corner-Point Grids. *SPE Journal*, 24 (4): 1552-1575.
7. Xu, Y., Cavalcante Filho, J.S.A., Yu, W., and Sepehrnoori, K. 2017. Discrete-Fracture Modeling of Complex Hydraulic-Fracture Geometries in Reservoir Simulators. *SPE Reservoir Evaluation & Engineering*, 20 (2): 403-422.
8. Xu, Y., Yu, W., and Sepehrnoori, K. 2019. Modeling Dynamic Behaviors of Complex Fractures in Conventional Reservoir Simulators. *SPE Reservoir Evaluation & Engineering*, 22 (3): 1110-1130.